Available online at www.sciencedirect.com
SCIENCE DIRECT
International Journal of Psychophysiology 61 (2006) 149 – 157
INTERNATIONAL JOURNAL OF PSYCHOPHYSIOLOGY
www.elsevier.com/locate/ijpsycho

Complex slow potential generators in a simplified attention paradigm

Luis F.H. Basile [a,b,*], Enzo P. Brunetti [a], José F. Pereira Jr. [a], Gerson Ballester [d,e], Edson Amaro Jr. [c], Renato Anghinah [a], Pedro Ribeiro [d,e], Roberto Piedade [d,e], Wagner F. Gattaz [a]

[a] *Department of Psychiatry, Faculty of Medicine, University of São Paulo, Brazil*
[b] *Faculdade de Psicologia e Fonoaudiologia, Universidade Metodistaa, Brazil*
[c] *Department of Radiology, Faculty of Medicine, University of São Paulo, Brazil*
[d] *Department of Neurosurgery, Faculty of Medicine, University of São Paulo, Brazil*
[e] *Department of Psychiatry, Federal University of Rio de Janeiro, Brazil*

Received 19 April 2005; received in revised form 16 September 2005; accepted 16 September 2005
Available online 28 November 2005

Abstract

We have recently obtained evidence for complex multifocal, individually variable generators of slow cortical potentials, elicited during performance of visual tasks involving expecting attention, comparison and memory [Basile, L.F.H., Ballester, G., Castro, C.C., and Gattaz, W.F., 2002. Multifocal slow potential generators revealed by high-resolution EEG and current density reconstruction. Int. J. Psychophysiol., 45 (3), 227–240; Basile, L.F.H, Baldo, M.V., Castro, C.C., and Gattaz, W.F. 2003. The generators of slow potentials obtained during verbal, pictorial and spatial tasks. Int. J. Psychophysiol., 48, 55–65]. The cue–target aspect of traditional paradigms for attention studies is equivalent to 'warning S1'–'imperative S2' in slow potential designs. We simplified Posner's spatial cueing task [Posner, M.I. 1980. Orienting of attention.Q. J. Exp. Psychol. Feb;32 (1), 3–25; Posner, M.I., Snyder, C.R., Davidson, B.J. 1980. Attention and the detection of signals. J Exp Psychol. Jun; 109 (2), 160–174] to temporal cuing only, by using visual cues to indicate the mere presence, on a known central position, of the eventual target (17 ms duration, ±0.3° grey circle). We recorded slow potentials on 12 healthy subjects, by 124-channel EEG system (Neuroscan Inc.), and modeled their generators using current density reconstruction (CDR) by L_p 1.2 norm minimization ("Curry V4.6", Neurosoft Inc.) applied to the target onset time. MRIs were obtained for each subject for constraining source models to individual brain anatomy. Average slow potentials were computed from above 60 artifact-free EEG-epochs (ISI=1.6 s, average ITI=2.5 s). We tabulated individual cortical current distributions by cytoarchitectonic area of Brodmann, after scaling into negligible, low, moderate and strong local density, based on percentile bands with respect to absolute maximum current. Despite the task's simplicity, the main result was individual variability and complexity in both scalp voltage and cortical current distributions. As observed in our previous studies, there was strong intersubject variability in the exact distribution of task-related cortical activity. Only parietal area 7 bilaterally was non-negligibly active in all subjects (currents above 10% maximum). As opposed to drawing conclusions based on group averaged data, we propose that activity by cytoarchitectonic area be ranked and statistically analysed only after being scaled on each individual. Based on the present results, the concept of a universal attention-related set of cortical areas if restricted to *common areas* across subjects is challenged, since even area 7 may no longer be common when the sample size becomes larger. We discuss the fact that group averaging may de-emphasize weakly but consistently active areas, and emphasize strongly but inconsistently active ones.

Keywords: Attention; Interindividual variability; Cortical electrical activity; High-resolution electroencephalography; Slow potentials; Functional mapping

1. Introduction

We have recently obtained evidence for generation of Slow Potentials (SPs) in multiple cortical association areas, during performance of a complex visual task including selective attention to verbal, pictorial and spatial stimuli, analysed by 124-channel EEG and Current Density Reconstruction (CDR) constrained by individual anatomy (Basile et al., 2002, 2003). SPs are a class of event-related potentials that includes the

* Corresponding author. Laboratory of Neuroscience (LIM-27), Department of Psychiatry, Faculty of Medicine, University of São Paulo. Av. Dr. Ovidio Pires de Campos s/n P.O. Box 3671 São Paulo, SP, 05403-010, Brazil. Tel.: +55 11 30697284, +55 11 32846821; fax: +55 11 2894815.
E-mail address: lbasile@usp.br (L.F.H. Basile).

0167-8760/$ - see front matter © 2005 Elsevier B.V. All rights reserved.
doi:10.1016/j.ijpsycho.2005.09.004

well-studied Contingent Negative Variations (CNVs; Walter et al., 1964; Walter and Crow, 1964; for a review, McCallum, 1988), which may now be considered a category of SPs restricted to simple motor tasks. In our previous experiments, the tasks included comparison of stimuli and memorization, beyond mere selective attention to the visual domains of interest. This could have explained one of our main overall findings, the large interindividual variability in the set of task-related active cortical areas. We developed a simple method emphasizing individual results, where group effects, including task-specific patterns, were obtained only *after* the scoring of electrical activity by cytoarchitectonic area in each experimental subject (Basile et al., 2003). This method has also proven itself useful when applied to a comparison between healthy and schizophrenic individuals (Basile et al., 2004).

In the present study, we intended to reduce the emphasis on comparison and memorization of stimuli, and to use a simple type of visual stimulus to reduce the perceptual complexity. Thus, starting from the type of paradigm standardized for (spatial) attention testing (Posner, 1980; Posner et al., 1980), we removed its spatial component by keeping both cue and possible target stimuli in the center of the visual field, maintaining only the probability aspect of Posner's paradigm (two possible cue stimuli with different validity). Thus, we used an exclusively temporal attention task, to simple visual targets. Our main aim was to verify whether in this case, by still analysing source reconstruction results on a case-by-case basis, a simpler and universally valid (across subjects) pattern of task-related cortical areas would be electrically active, corresponding to this target expectancy SP.

2. Methods

2.1. Subjects

Twelve healthy individuals with normal vision and hearing, 9 male and 3 female, participated in the study. They ranged in age between 20 and 45 years, with no history of drug or alcohol abuse, and no current drug treatment. All subjects signed consent forms approved by the Ethics Committee of the University of São Paulo Hospital.

2.2. Stimuli and task

A commercial computer program (Stim, Neurosoft Inc.) controlled all aspects of the task. Visual stimuli composing the cue–target pairs (S1–S2) consisted in small rectangles (vertical or horizontal central visual filled black rectangles, excentricity ±0.8°, 100 ms duration were the two possible types of S1 stimuli). The vertical and horizontal S1 rectangles corresponded, respectively, to 75% or 25% probability of occurrence of the target, i.e., *presence, on the known central position,* inside the S2 rectangle, of a ±0.3° grey circle target, with a duration of only 17 ms. S1 was followed by S2, with onsets *separated in time* by 1.6 s. We used such cue validity probabilities to maintain the similarity with Posner's task in this respect, and because they are supposed to maximize expecting attention and their correlates (McCallum, 1988): probabilities close to 50% mean no validity, and close to 100% would transform the task into mere time estimation. We instructed the subjects that *a rectangle* would be presented to indicate that 1.6 s later it would flash again but quickly, containing or not the target circle. No instructions were given regarding target probabilities. The subject decided whether there was a target inside the S2 rectangle, and indicated presence of target by pressing the right button with the right thumb or absence of target by pressing the left button with the left thumb. We explicitly de-emphasized reaction time in the instructions and measured performance exclusively by the percent correct trials, from the total of 96 trials comprising the experiment. An eye fixation dot was continually present on the center of the screen, as well as a stimulus-masking background, to prevent after-images.

2.3. Recordings, computation of average potentials and acquisition of MRIs

We used a fast Ag/AgCl electrode positioning system consisting of an extended 10–20 system, in a 124-channel montage (Quik-Cap, Neuromedical Supplies®), and an impedance-reducing gel which eliminated the need for skin abrasion (Quick-Gel, Neuromedical Supplies®). Impedances usually remained below 3 kΩ, and channels that did not reach those levels were eliminated from the analysis. To know the actual scalp sampling or distribution of electrodes in each individual with respect to the nervous system, we used a digitizer (Polhemus®) to record actual electrode positions with respect to each subject's fiduciary points: nasion and preauricular points. After co-registration with individual MRIs, the recorded coordinates were used for realistic 3D mapping onto MRI segmented skin models, and later used to set up the source reconstruction equations (distances between each electrode and each dipole supporting point). Two bipolar channels, out of the 124 channels in the montage were used for recording both horizontal (HEOG) and vertical electrooculograms (VEOG). Linked mastoids served as reference only for data collection (common average reference was used for source modeling) and Afz was the ground. We used four 32-channel DC amplifiers (Synamps, Neuroscan Inc.) for data collection and the Scan 4.0 software package (Neurosoft Inc.) for initial data processing (until computation of averages). The filter settings for acquisition were from DC to 50 Hz, and the digitization rate was 250 Hz. The EEG was collected continuously, and epochs for averaging spanned the interval from 300 ms before S1 to 400 ms after S2 presentation. Baseline was defined as the 300 ms preceding S1. Artifact elimination was automatic: epochs containing signals in either HEOG or VEOG channels above +50 or below −50 μV were eliminated. In our montage, the VEOG detected blinks as deflections above 130 μV in the positive direction.

MRIs were obtained by a 1.5 Tesla GE machine, model Horizon LX. Image sets consisted in 124 T1-weighed saggital images of 256 by 256 pixels, spaced by 1.5 mm. Acquisition parameters were: standard echo sequence, 3D, fast SPGE, two

excitations, RT=6.6 ms, ET=.6 ms, flip angle of 15°, F.O.V=26 × 26 cm^2. Total acquisition time was around 8 min.

2.4. Intracranial source reconstruction

The computed average SPs, MRI sets and electrode position digitization files were the raw data for all further analysis (Curry V 4.6, Neurosoft Inc.). The first critical step in the source analysis was the estimation of noise in the data, whose criterion was the standard deviation in the amplitudes of points comprising the 300 ms baseline. In all cases the noise thus computed was below 1 μV (typically below 0.6 μV). For all subsequent analysis, the electrical data were converted to absolute numbers, i.e., signal to noise ratios (SNR) on individual channels with respect to the average noise level computed for each recording session. In pilot studies, we have performed systematic tests on the effects of various criteria of noise definition (baseline, cross-channel average or individual channel 20% lowest amplitude data points) on the resulting SNRs and source reconstruction. The most pessimistic criterion in each case, when compared to the baseline criterion, results in at most double the overall noise level. The corresponding estimated SNR definitions lead to a set of virtually identical topographic distributions of data, therefore to identical source models with respect to relative current density distribution.

For the inclusion of a 'noise component' into the source model itself, the physical unit-free or 'standardized' data (with retained polarity) were decomposed by Independent Component Analysis (ICA), which searches for the highest possible statistical independence or redundancy reduction between components (in this case, spatio-temporal averaged data patterns), a robust method of blind signal decomposition/deconvolution (for a review see, e.g. Hyvarinen and Oja, 2000). ICA was applied to each individual's whole space–time data set, i.e., to the $m \times n$ data matrix (m used channels times 475 time samples corresponding to the 1.6 s interval from the onset of S1 to that of S2 plus baseline). Finally, we fed the reconstruction algorithm with the main ICA component(s) as data to be fitted (in our studies, the SPs invariably correspond to the first component, and evoked potentials usually to second through fourth). Thus, the 'noise component' of the model was defined as the sum of remaining components (with loadings below SNR=1), which at the time point of interest lead invariably to negligible scalp potentials, due to absence of the evoked potentials that also have loadings above SNR=1. Such noise component is required by any CDR method for setting up the inconsistent system of equations that relate sources with measured data. Otherwise, a system identical to zero (vector) would result in solutions that rely excessively on the actual measurements, being subject to important distortions by outlying values and any form of experimental error. MRI sets were linearly interpolated to create 3-dimensional images, and semi-automatic algorithms based on pixel intensity bands served to reconstruct the various tissues of interest. A Boundary Element Model (BEM) of the head compartments was implemented, by triangulation of collections of points supported by the skin, skull and cerebrospinal fluid (internal skull) surfaces. Mean triangle edge lengths for the BEM surfaces were, respectively, 10, 9 and 7 mm. Fixed conductivities were attributed to the regions enclosed by those surfaces, respectively, 0.33, 0.0042 and 0.33 S/m. Finally, a reconstructed brain surface, with mean triangle side of 3 mm, served as the model for dipole positions, corresponding to approximately 20 thousand points. The electrode positions were projected onto the skin's surface following the normal lines to the skin. The detailed description of the assumptions and methods used by the "Curry 4.6" software for MRI processing and source reconstruction may be found elsewhere (Curry 4.0 User Guide, 1999; or e.g., Buchner et al., 1997; Fuchs et al., 1998, 1999).

The analysis program then calculated the lead field matrix that represents the coefficients of the set of equations which translate the data space (SNR values in the set of channels per time point) into the model space (the approximately 20 thousand dipole supporting points). The large number of dipole support points used in CDR must not be confused with "sources" that explain each ICA component of sufficient SNR: For modeling each component, one may choose either a single dipole or a 'continuous distribution' of current density, which is approached by a large number of dipoles. In the present study, each high SNR component found, out of which only the first is of interest, was modeled by CDR as an extended, not necessarily contiguous source. The source reconstruction method itself was L_p norm minimization, with $p=1.2$ both for data and model terms. The regularization factor, or λ values to be used, typically converged after repeating the fitting process three to four times. Lambda is the numeric factor that weighs the model term, one of the two terms of the reconstruction problem: the second or data term is the set of equations whose solution approaches the model (intracranial current densities) to the measured data. Since both terms are minimized simultaneously, λ gives the balance between goodness of fit and model size:

$$\Delta^2 = |D_{(j)}|^p + \lambda |M_{(j)}|^p,$$

where Δ^2 is the extended variance, $D(j)$ or data term equals $L_j - m$ (L is the lead field matrix, j is the current vector per time point and m is the measured data vector), and $M(j)$ is the model term, which in this case is a measure of the "size", or scalar sum of all current strengths. All CDR methods are more realistic than single or few dipoles modeling when applied to SPs or endogenous potentials, since they allow extended instead of punctiform sources (which have to be considered unevenly weighed centers of current density; discussion and references in Basile et al., 1996, 1997). However, each method has its own shortcomings, L_p norm minimization leading to unstable (with respect to noise estimation) absolute current values. This is not a problem to our applications, since we are interested exclusively in the relative topographic and current density distribution. Of course, CDR methods are also not decisive with respect to the generators of any scalp recorded potentials, which could

only be known if a vast invasive sampling of cortical areas were used. But once more, the important point here is that we use a common method across subjects.

Resulting models were inspected with respect to the individual anatomy directly, a straightforward procedure allowed by our software. Foci of current density were analyzed in terms of which cytoarchitectonic areas they covered, after being separately defined or isolated by the application of various percentile cutoff values (see below). The Brodmann areas containing current foci were tabulated after verification by comparison with classical illustrations and the conventional Talairach and Tournoux atlases (1988).

2.5. Scoring of relative current density and statistical analysis

Our approach to translate the complexity of current distribution into quantifiable results for overall analysis was a recently implemented method that avoids collapsing of the original data into an "universal", model brain, thus preserving individual anatomical and functional (electrical)

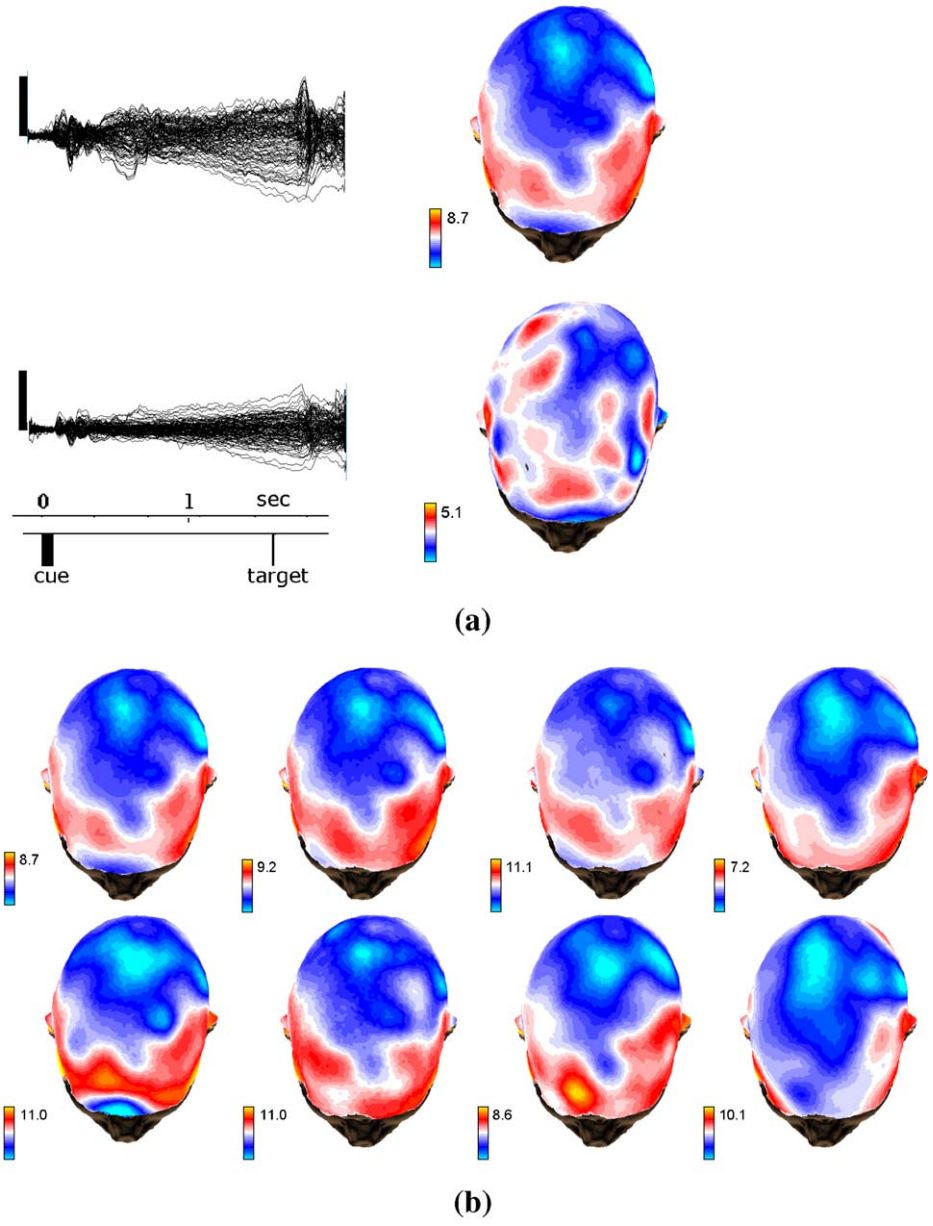

Fig. 1. (a) Example from one individual (left) and grand averaged data (below), of average SPs and corresponding isopotential topographic maps (right). Waveforms from all channels are superimposed, with common baselines. Isopotential maps corresponding to group averaged data (collapsed across the montage, were used only for illustration purposes) are projected over the scalp of an individual of median head size (same from above). Potentials calculated with respect to 'common average reference electrode'. Task events are indicated below (S1–S2 interval). Vertical bar at left of upper waveforms indicate 10 μV. (b) Topographic maps from same example individual as in panel (a), computed with different number of randomly chosen epochs. At upper left, $n=80$; three remaining upper row maps, $n=40$; maps at bottom row, $n=20$, mutually exclusive epochs. Numbers at right of color bars indicate voltage level of extreme colors (yellow — positive, magenta — negative extremum level). Notice preservation of isopotential lines across averages, especially where high potential gradients are found, such as isopotential=0 (area in white). (For interpretation of the references to colour in this figure legend, the reader is referred to the web version of this article.)

information (Basile et al., 2003, 2004). We scored relative current densities by cortical cytoarchitectonic area into four levels (negligible, low, moderate and high), using percentile bands relative to maximum current, defined by fixed cutoff levels. We inspected current density results in each cortical area after applying a set of percent cutoff values from each data set's maximum current value. Cortical areas containing current density foci of intensity above 70% of the maximum were given a relative electrical activity score 4 (high). Activity between 40% and 70% was considered of moderate intensity and given a score 3, between 10% and 40% low and given a score 2, and below 10% of the maximum was considered negligible and given a score 1. Then, scores in each cytoarchitectonic area were tabulated for the verification of common or variable current distribution patterns.

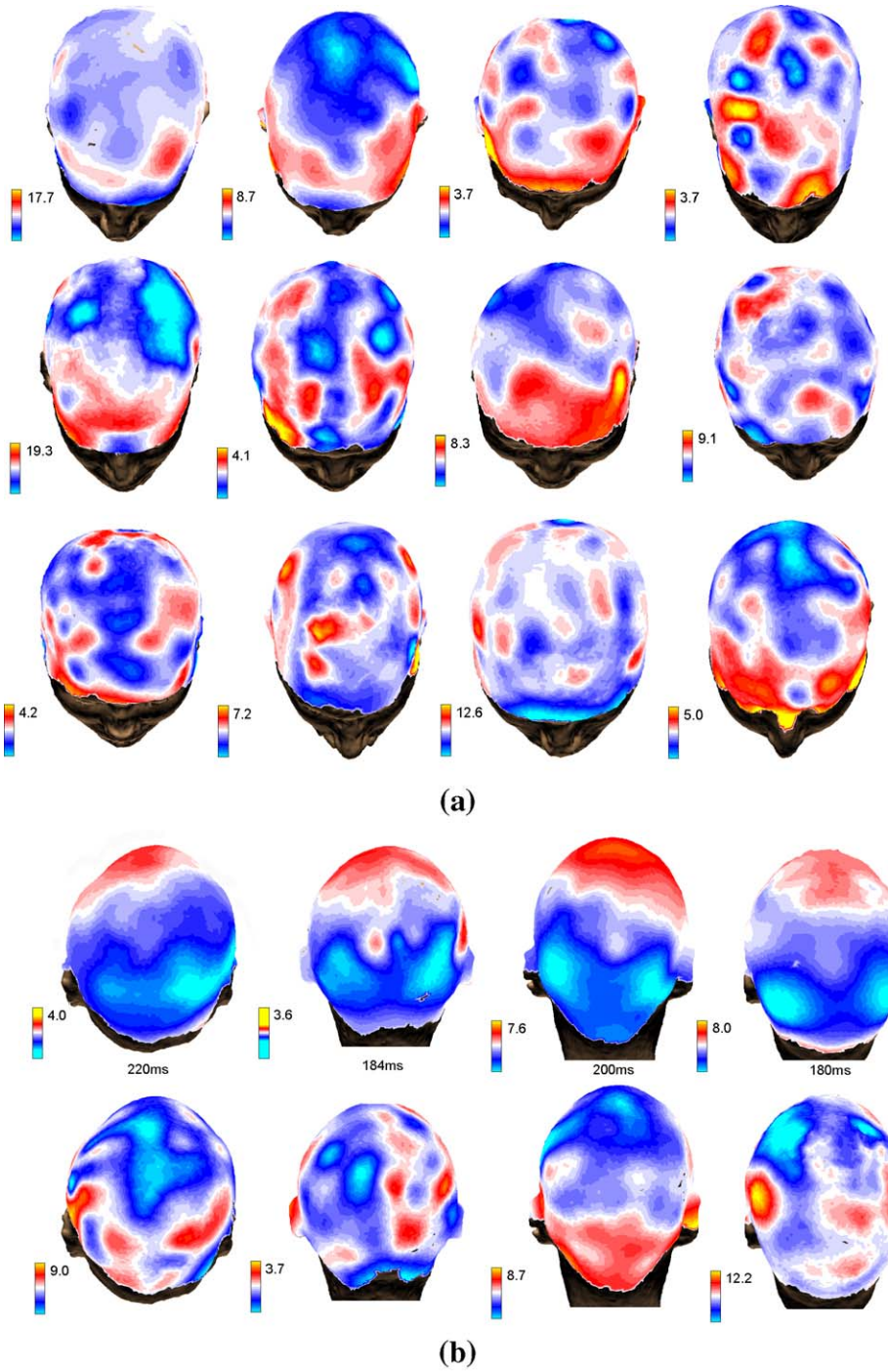

Fig. 2. (a) Topographic maps at point of S2 onset, from all subjects. (b) Topographic maps at peak of the visual N200 from four example subjects (upper row; numbers below maps indicate time of N200 peak in ms), and of slow potentials (S2 onset) seen from the same angle (bottom row). Numbers at right of color bars indicate voltage level of extreme colors (yellow — positive, magenta — negative extremum level). (For interpretation of the references to colour in this figure legend, the reader is referred to the web version of this article.)

3. Results

All subjects reported that effort of attention to the S1–S2 pairs was necessary for detection of targets, in which case performance was relatively easy. The overall average performance was 88.5% correct responses (standard deviation = 8.3%). It is important to mention that *none of the subjects* did notice a difference between vertical and horizontal rectangles with respect to presence of targets, when explicitly asked. This was surprising to us and may indicate a common aspect in task strategy, according to their point of view, i.e., they were simply expecting for the targets at S2.

All subjects presented slow potentials for the task, of typical maximum amplitudes of above 5 μV at the onset of S2: group mean maximum amplitude to common average reference was 5.3 (±1.9) μV; as a global amplitude measure, we computed the square root of mean global field power, whose group mean was 3.7 (±1.1) μV. The mean noise level across subjects was 0.55 (±0.16) μV, corresponding to mean SNR value of 6.3 (±3.9) at the onset of S2 (worst estimated mean noise was 0.96 (±0.16) μV). High impedance channels were dispersed across the montage, that is, in no case did they form a contiguous gap in the montage, and ranged between 5 and 12 across subjects. We used the criterion of a minimum of 60 epochs to compute SPs (which included all subjects), but most subjects lost fewer than 10 epochs due to eye artifacts. Averages were computed irrespective of performance, thus including the fewer epochs followed by error, since our main interest was in the SPs, which are correlates of anticipation, and in the mere attempt to perform the task. Fig. 1(a) shows an example of individual electrical data set, and the grand averaged data projected on a median head subject (computed by collapsing the data across subjects in the common montage, only for illustration purposes and not used for further conclusions). Notice the complexity of voltage distribution on the scalp (of high gradient and positive voltage regions surrounding the negative voltage central area), as

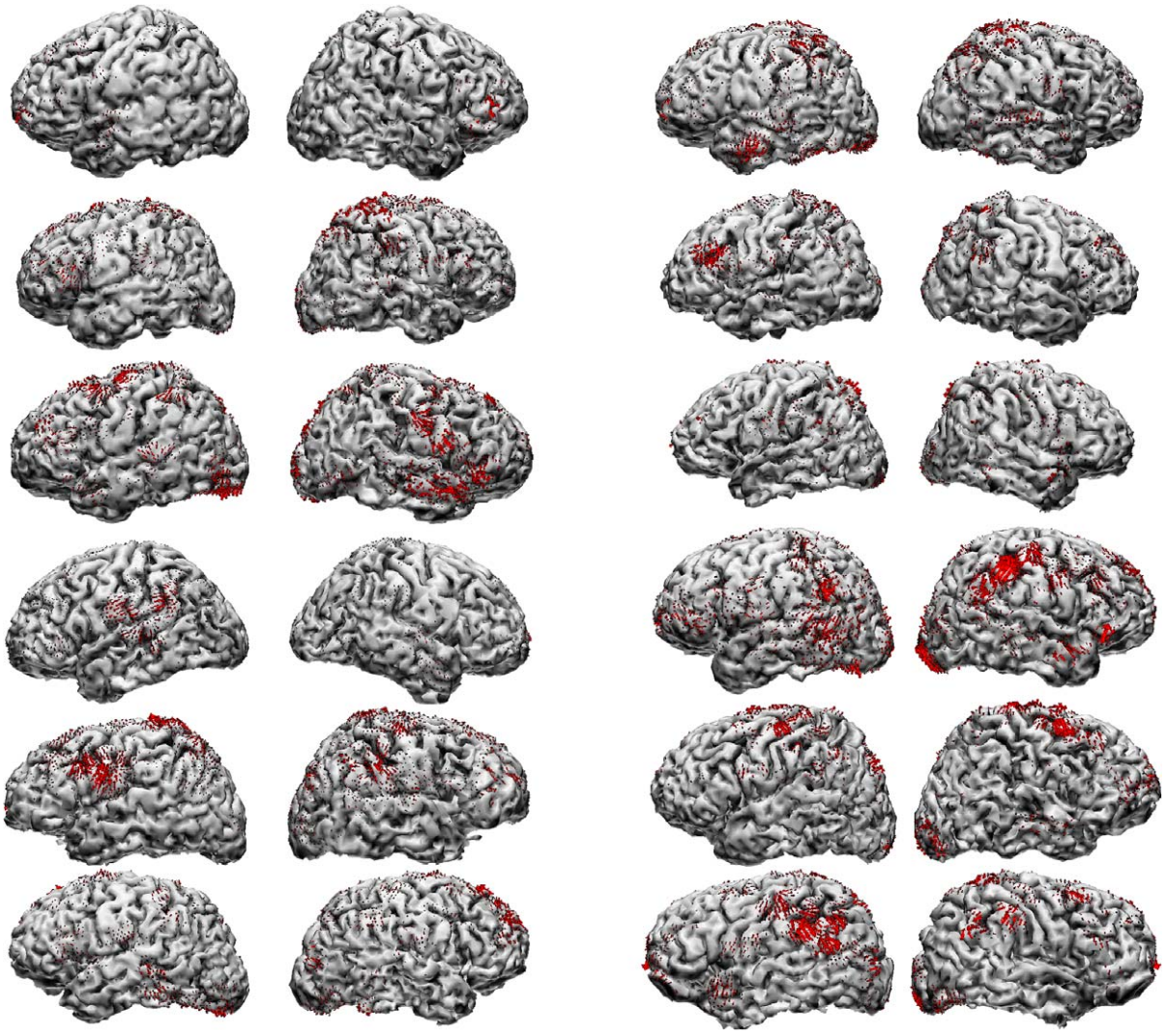

Fig. 3. Current density reconstruction results for all subjects. Current density indicated by small red arrows, (arrow size proportional to local current density). Currents shown, above 10% of individual current density maxima, including low, moderate and high intensities, respectively, with scores 2, 3 and 4). (For interpretation of the references to colour in this figure legend, the reader is referred to the web version of this article.)

compared with more familiar sensory evoked potentials, for instance. Notice also the relative reduction of voltage for grand averaged data, which is a finding common to our previous studies, and in itself an indication of topographic variability across subjects. The topography of SPs for all subjects at the point of analysis is shown in Fig. 2(a). To reassure that the SP complexity and variability were not due to within subject data instability, we have reaveraged the data of each subject using a range of a smaller number of randomly chosen epochs. The topography of SPs thus averaged demonstrated a clear intraindividual stability, typically when between 20 and 30 epochs were used, and is exemplified in Fig. 1(b). We have also verified that, in spite of the weak visual stimulation used in the experiment, the evoked potentials computed from the same data set do demonstrate the expected invariability across subjects. Fig. 2(b) shows the variable SP distribution from the same angle that best presents similar visual N200 topographies in four subjects. As in our previous studies, although ICA was used only as a necessary step for defining 'noise components' for CDR, we again verified that, in all cases, the first component, when separated from the remaining ones by ICA weighed filtering, had the time course and scalp distribution virtually identical to the SPs.

Current density reconstruction results also had a correspondingly complex form. In all subjects and conditions, we observed a complex, multifocal pattern of current density foci. Fig. 3 presents the reconstruction results, in all individuals, plotted for currents above 10% of individual maximum. In this present case, visual inspection alone is enough for the main conclusion regarding the complexity and individual variability in active cortical areas across subjects. In any case, many areas were observed to most frequently contain non-negligible (above 10% of maximum density) current density foci, one of which common to all subjects. Thus, only parietal area 7 bilaterally, contained non-negligible current density foci in all subjects. As in previous studies also, the commonly active are not necessarily strongly active across subjects, as well as strongly active areas in most subjects are not the ones common to all. Thus, for instance, when ranked according to overall scores (Fig. 4), right frontal areas 10 and 9, inactive in only one subject each, are preceded, aside from both areas 7, by seven other areas, among which area 6 bilaterally, left 40 and right 5, each inactive in two subjects.

4. Discussion

The SPs obtained in all subjects were once more observed to be complex in distribution over the scalp, as in our recent studies using a more complex paradigm (Basile et al., 2002, 2003). Both in those studies and in the present one, the generators of SPs have a multifocal distribution comprising mainly association cortices from prefrontal and posterior areas. Methodological biases do not explain the topographic and corresponding CDR variability across subjects: The arbitrary choice points in the analysis such as noise estimation and definition of relative current intensity levels in our scoring method, maintained the topography of individual results unaltered, except for absolute values. If SNR values were low (which is not the case even in the most pessimistic estimation), unstable individual results could be expected, i.e., large intraindividual variability on replications. This was ruled out by the direct verification of SP stability during reaveraging using fewer randomly chosen EEG epochs for each subject, and verification of the expected similarity of early evoked potential topography across subjects on the same data set. Finally, although CDR itself is of a mathematical model nature, it is a common procedure across subjects, based on the more trustable scalp topographic data which is itself more trustable and clearly variable between individuals.

Qualitatively, this type of result agrees with the typical results from metabolic tracing studies, when individual cases are analysed, such as fMRI and PET (e.g., Cohen et al., 1996; Fink et al., 1997; Davis et al., 1998; Brannen et al., 2001; Tzourio-Mazoyer et al., 2002). This type of variability is a common observation in studies using most types of tasks, excepting only studies of simple voluntary sensorimotor activity (Fink et al., 1997), although even some studies on passive stimulation do emphasize variability (Davis et al., 1998; Hudson, 2000). An unavoidable variability in task performance strategy across subjects is a commonly claimed explanation for variable cortical ensembles activity during any given task. In spite of the relatively simple task used, at least from the point of view of subjects, such possibility still cannot be ruled out: Although all subjects reported a simple expectation to see the target and did not notice the different occurrence of targets between S1 types, those two conditions and the arbitrary mapping of either thumb's motor response onto absence or presence of target could add some diversity in strategies. Especially so, if strategy variability is indeed an

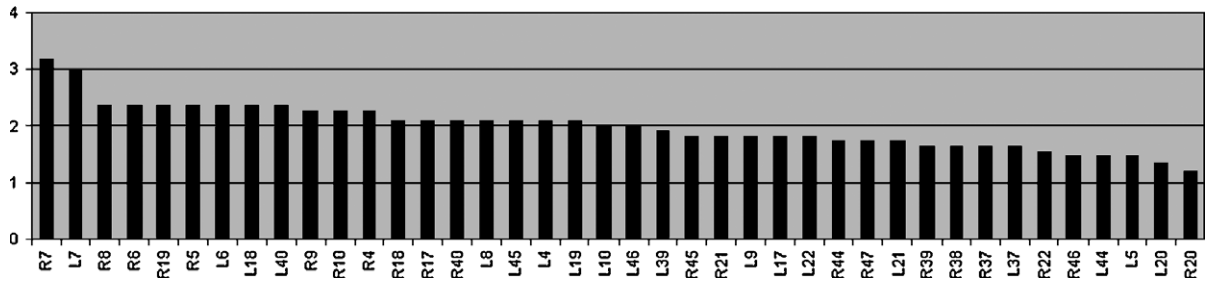

Fig. 4. Average, across subjects, of cortical activity scores by cytoarchitectonic areas of Brodmann (R = right; L = left) where, in each subject, either negligible, weak, moderate or strong currents were observed (respectively, with scores 1, 2, 3, 4).

unavoidable human attribute, and regards some neural process independent from subjective experience which can hardly be expected to vary as much in the present case. More extreme possibilities still cannot be ruled out as well: The extent and complexity of cortico-cortical connections between associative areas could allow the formation of individual-specific complex functional network interactions during learning of any given task including, at least in principle, even 'superfluous' or 'colateral' areas, i.e., areas whose removal from the set would not affect performance. But those collateral pathways would become critical in large-scale functional plasticity and recovery of function. This idea is included in the more embracing concept of biological degeneracy (Edelman and Gally, 2001), thoroughly discussed as applied to task performance and recovery of function by Noppeney et al. (2004). Finally, we have no reason at the present to claim a simple, one-to-one mapping between strategy, psychological experience and set of active cortical areas during any given task execution. By means of the concepts of neural degeneracy and its counterpart, pluripotentiality, Noppeney et al. (2004) explicitly propose alternative forms of mapping between task performance and nervous system subcomponents.

Most recent studies such as the ones cited above, from the last decades, have produced a vast literature on task-related brain changes using results averaged across subjects. We suggest, as some other authors also explicitly do (Steinmetz and Seitz, 1991; Davis et al., 1998; Noppeney et al., 2004), that any functional mapping study take into consideration individual data, before any functional claims regarding specific cortical areas are attempted (see discussions in Basile et al., 2003; Noppeney et al., 2004). By averaging, the presently observed weakly but consistently (across individuals) active areas are de-emphasized, and reciprocally, strongly active areas in some subjects which are not common to all may be excessively emphasized and become erroneously claimed as essential for particular functions. In the case of physiopathological studies, the need for individual analysis is becoming increasingly acknowledged. For example, a study of SPs in schizophrenia provided evidence for a multifocal cortical *dysfunction* (Basile et al., 2004), as opposed to the long claimed 'hypofrontality', which could be observed even by the averaging of *unequal hyperfunctional* prefrontal areas across subjects (various hypotheses explaining controversial findings in schizophrenia are reviewed by Manoach, 2003). Whereas in schizophrenia clinical subtypes would add a 'supraindividual' level of variability, an even higher degree of variability is expected 'within subjects', in the case of functional reorganization after focal brain lesions (Noppeney et al., 2004).

Only parietal area 7 bilaterally presented non-negligible activity in all subjects. Studies on the role of area 7 in selective attention to interesting objects have been exceptionally replicated, since the first single-cell electrophysiological studies on monkeys (Lynch et al., 1977; Yin and Mountcastle, 1978).

It is hard to conceive of a task in which a more universal pattern of electrical activity across individuals may be observed, if dependent upon our ideas regarding simplicity of design, since anticipated target detection appears to be a minimal component of any voluntary task. The target stimulus, on its turn, should not be expected to generate highly variable activity corresponding to perceptual representation (in posterior cortices), due to its simplicity and restriction to the central fovea.

We are currently analyzing results and applying variations of the same visual task used here (distractors, passive conditions, dual-task conditions, and alternative tasks) in the same set of individuals, to verify the stability of results, degrees of attention with respect to sources, the possible commonality or difference in source distribution between modalities (auditory), and the possible emergence of different patterns and rhythms (theta and delta range) with increased effort. Encouraging preliminary results suggest that passive attention to the same stimuli after task performance, but in that case without task engagement, results in very similar, equally complex and individually specific source distributions, only with smaller amplitudes. They also suggest a predominantly common set of active areas between the individually specific present results, and results for SPs to an analogous auditory task.

Acknowledgments

This research was supported by the grants 03/02297-9 and 02/13633-7 from Fapesp, São Paulo, Brazil.

References

Basile, L.F.H., Simos, P.G., Brunder, D.G., Tarkka, I.M., Papanicolaou, A.C., 1996. Task-specific magnetic fields from the left human frontal cortex. Brain Topogr. 9 (1), 31–37.

Basile, L.F.H., Rogers, R.L., Simos, P.G., Papanicolaou, A.C., 1997. Magnetoencephalographic evidence for common sources of long latency fields to rare target and rare novel stimuli. Int. J. Psychophysiol. 25, 123–137.

Basile, L.F.H, Ballester, G., Castro, C.C., Gattaz, W.F., 2002. Multifocal slow potential generators revealed by high-resolution EEG and current density reconstruction. Int. J. Psychophysiol. 45 (3), 227–240.

Basile, L.F.H, Baldo, M.V., Castro, C.C., Gattaz, W.F., 2003. The generators of slow potentials obtained during verbal, pictorial and spatial tasks. Int. J. Psychophysiol. 48, 55–65.

Basile, L.F.H., Yacubian, J., deCastro, C.C., Gattaz, W.F., 2004. Widespread electrical cortical dysfunction in schizophrenia. Schizophr. Res. 69, 255–266.

Brannen, J.H., Badie, B., Moritz, C.H., Quigley, M., Meyer, M.E., Haughton, V.M., 2001. Reliability of functional MR imaging with word-generation tasks for mapping Broca's area. AJNR Am. J. Neuroradiol. 22 (9), 1711–1718.

Buchner, H., Knoll, G., Fuchs, M., Rienacker, A., Beckman, R., Wagner, M., Silny, J., Pesch, J., 1997. Inverse localization of electric dipole current sources in finite element models of the human head. Electroenceph. Clin. Neurophysiol. 102 (4), 267–278.

Cohen, M.S., Kosslyn, S.M., Breiter, H.C., DiGirolamo, G.J., Thompson, W.L., Anderson, A.K., Brookheimer, S.Y., Rosen, B.R., Belliveau, J.W., 1996. Changes in cortical activity during mental rotation. A mapping study using functional MRI. Brain 119 (Pt 1), 89–100.

Davis, K.D., Kwan, C.L., Crawley, A.P., Mikulis, D.J., 1998. Functional MRI study of thalamic and cortical activations evoked by cutaneous heat, cold, and tactile stimuli. J. Neurophysiol. 80 (3), 1533–1546 (Sep).

Edelman, G.M., Gally, J.A., 2001. Degeneracy and complexity in biological systems. Proc. Natl. Acad. Sci. U.S.A. 98 (24), 13763–13768. (Nov 20).

Fink, G.R., Frackowiak, R.S., Pietrzyk, U., Passingham, R.E., 1997. Multiple nonprimary motor areas in the human cortex. J. Neurophysiol. 77 (4), 2164–2174.

Fuchs, M., Wagner, M., Wischmann, H.A., Kohler, T., Theissen, A., Drenckhahn, R., Buchner, H., 1998. Improving source reconstructions by combining bioelectric and biomagnetic data. Electroencephalogr. Clin. Neurophysiol. 107 (2), 93–111.

Fuchs, M., Wagner, M., Kohler, T., Wischmann, H.A., 1999. Linear and nonlinear current density reconstructions. J. Clin. Neurophysiol. 16 (3), 267–295.

Hudson, A.J., 2000. Pain perception and response: central nervous system mechanisms. Can. J. Neurol. Sci. 27 (1), 2–16 (Feb).

Hyvarinen, A., Oja, E., 2000. Independent component analysis: algorithms and applications. Neural Netw. 13 (4–5), 411–430.

Lynch, J.C., Mountcastle, V.B., Talbot, W.H., Yin, T.C., 1977. Parietal lobe mechanisms for directed visual attention. J. Neurophysiol. 40 (2), 362–389.

Manoach, D., 2003. Prefrontal Cortex Dysfunction During Working Memory Performance in Schizophrenia: Reconciling Discrepant Findings.

McCallum, WC., 1988. Potentials related to expectancy, preparation and motor activity. In: Picton, T.W. (Ed.), Handbook of Electroencephalography and Clinical Neurophysiology, Human Event-Related Potentials revised series, vol. 3. Elsevier, pp. 427–534.

Noppeney, U., Friston, K.J., Cathy, J., 2004. Price degenerate neuronal systems sustaining cognitive functions. J. Anat. 205, 6.

Posner, M.I., 1980. Orienting of attention. Q. J. Exp. Psychol. 32 (1), 3–25 (Feb).

Posner, M.I., Snyder, C.R., Davidson, B.J., 1980. Attention and the detection of signals. J. Exp. Psychol. 109 (2), 160–174. (Jun).

Steinmetz, H., Seitz, R.J., 1991. Functional anatomy of language processing: neuroimaging and the problem of individual variability. Neuropsychologia 29 (12), 1149–1161.

Talairach, J., Tournoux, P., 1988. Co-planar Stereotaxic Atlas of the Human Brain. Thieme Medical Publishers, Inc., New York.

Tzourio-Mazoyer, N., Josse, G., Crivello, F., Mazoyer, B., 2002. Interindividual variability in the hemispheric organization for speech. Neuroimage 16 (3), 765–780.

Walter, W.G., Crow, H.J., 1964. Depth recording from the human brain. Electroenceph. Clin. Neurophysiol. 16, 68–72.

Walter, W.G., Cooper, R., Aldridge, V.J., McCallum, W.C., Winter, A.L., 1964. Contingent negative variation: an electric sign of sensorimotor association and expectancy in the human brain. Nature 203, 380–384.

Yin, T.C., Mountcastle, V.B., 1978. Mechanisms of neural integration in the parietal lobe for visual attention. Fed. Proc. 37 (9), 2251–2257.